Electronic Journal «Technical Acoustics»
http://www.ejta.org

2009, 14

Panagiota Marazioti

Dept. of Energy Technology, Technological Education Institute (TEI), Athens, Greece;
Dept. of Mechanical and Aeronautics Engineering, University of Patras, Greece 26 500,
e-mail: emaraziot@upatras.gr

Computational fluid dynamics modeling of the combustion noise (roar) in attached-lifted propane jet diffusion flames and comparison of the numerical results

Received 15.09.2009, published 12.11.2009

The autonomous noise generation by the turbulence interactions, heat release and chemistry fluctuation in front of an attached propane jet diffusion flame was investigated numerically. In the computational procedure the Large Eddy simulation turbulent model (LES) was employed to calculate the reacting jet flows. A reactedness-mixture fraction two-scalar exponential probability density function (PDF) model based on non-premixed flame arguments was used. The preliminary results of the computational fluid dynamics model (CFD) suggest that the location of the maximum noise intensity coincides with the region of the peak temperatures levels. The lifted flame gives elevated energy content in the sound spectrum than the attached one and the difference in the noise level is about 40 dB at most frequencies and mostly near the frequency 80 Hz. The present methodology has been certificated through a series of experimental measurements and a reasonable agreement was observed. It is believed that the present procedure has captured the basic behaviors and trends in the aero-thermochemical and flame noise generation characteristics, of the studied jet diffusion flames, although further tests and improvements would be required to enlarge the applicability of the method.

Key words: combustion roar, attached flame, autonomous noise, sound spectrum, turbulent combustion modeling.

1. INTRODUCTION

The integrated Combustion Control approach through artificial recognition and manipulation of the combustion-generated noise has recently been put forward as a methodology suitable to offers important impulse in the optimisation of functional behaviour modern systems of combustion chamber with important profits in the cost and in the safety. Combustion roar is related to the noise generated directly by the flame due to turbulent fluctuations independently or in combination with acoustic resonance with the reacting environment and usually involves a broadly distributed spectrum [1–4].

The topic is of interest to practical combustor designs since it is interrelated with combustor acoustic/pressure oscillations or resonance, acoustic pollution of the environment

diagnosis of operational variations and faults and ultimately active or hybrid combustor operation control techniques. Practical examples which are interesting from the point of view of research into combustion roar is the combustion chambers of aircraft jet engines, flares and hot-air balloons where minimization of flame noise is desirable.

To describe the acoustic performance of the jet flame as autonomous source of sound an integral expression is employed that provides the (acoustically one-dimensional) noise spectrum from the flame in terms of an assumed shape turbulence spectrum at the flame front closely following the formulation put forward and derived in closed form by [5–7].

As a first step towards understanding the phenomenon turbulent non-premixed jet flames lifted from the burner rim are studied as model problems. A diffusion flame attached to the burner nozzle lifts above the jet exit rim or blows out abruptly when the fuel jet velocity steadily increases and exceeds a critical value [8, 9]. Apart from their relevance in the design and safe operation of industrial systems such jet flame stability phenomena provide a useful research tool for experimental and numerical studies of turbulent reacting flow characteristics and related phenomena such as those presently addressed. Non-intrusive measurements by Schneider, et al. [10] suggest that individual theories such as turbulent premixed flame propagation, laminar flameless quenching, large or small scale mixing are all plausible theoretical viewpoints to describe the coupled aerothermochemical phenomena of lift-off and blow-out.

In the described work a two-dimensional time-dependent phase-averaged Navier-Stokes flow simulation method capable of calculating the mean and turbulent properties of the momentum and thermo-chemical fields is employed to study the behavior of axisymmetric co-flowing methane-air attached jet diffusion flame configuration [11-13]. Both laminar and turbulent (lifted-off) operational conditions have been investigated to test and develop the model over a range of conditions with increasing complexity. A modular post-processor is then employed for the prediction of turbulent combustion noise exploiting the time-mean and fluctuating thermo-chemical quantities obtained from the basic reacting flow field predictions.

2. MODEL SIMULATION

2.1. Combustion model (basic turbulence/chemistry interaction model)

A partial equilibrium scheme corresponding to a two-scalar description employing the mixture fraction, f, and the CO_2 concentration, Y_{CO_2}, were used. The reaction $CO + OH \leftrightarrow CO_2 + H$ was introduced to allow for non-equilibrium effects and CO_2 formation from CO is assumed to proceed as:

$$\dot{r}_{co_2} = k_f Y_{CO} Y_{OH} - \left(\frac{k_f}{k_\varepsilon}\right) Y_{CO_2} Y_H, \quad k_f = 6.76 \cdot 10^{11} \exp\left(\frac{T}{1102}\right) \tag{1}$$

and k_ε is taken from the JANAF (Tables).

Additionally when the mixture strength exceeds the rich flammability limit the composition is taken as that of equilibrium at this limit diluted with pure fuel. The final

composition is calculated from the NASA equilibrium code for given f and Y_{CO_2} values by defining Y_{CO_2} as an 'element'. The passive, f, and the reactive, Y_{CO_2}, variables, are calculated from the equations (2, 3) with $\overline{\rho}$ average density, $\widetilde{u}_j$, $\widetilde{f}$ and $\widetilde{Y}_{CO_2}$ Favre average and gradient

$$\frac{\partial\left(\overline{\rho}<\widetilde{f}>\right)}{\partial t}+\frac{\partial}{\partial\chi_j}\left(\overline{\rho}<\widetilde{u}_j><\widetilde{f}>\right)=\frac{\partial}{\partial\chi_j}\left[\left(\overline{\rho}D+\frac{\mu_t}{S_{C_t}}\right)\frac{\partial<\widetilde{f}>}{\partial\chi_j}\right], \tag{2}$$

$$\frac{\partial\left(\overline{\rho}<\widetilde{Y}_{CO_2}>\right)}{\partial t}+\frac{\partial}{\partial\chi_j}\left(\overline{\rho}<\widetilde{u}_j><\widetilde{Y}_{CO_2}>\right)=\frac{\partial}{\partial\chi_j}\left[\left(\overline{\rho}D+\frac{\mu_t}{S_{C_t}}\right)\frac{\partial<\widetilde{Y}_{CO_2}>}{\partial\chi_j}\right]+\overline{\rho}\widetilde{r}_{CO_2} \tag{3}$$

transport assumptions for the turbulent fluxes $\overline{u_j' f'}$ and $\overline{u_j' Y_{CO_2}'}$.

An exponential joint PDF is constructed from the normalized mixture fraction and CO_2 concentration values, f^* and $Y_{CO_2}^*$, which are used to transform the physically allowable space of f and Y_{CO_2} into a normalized square area suitable for integration. The relationships established by this transformation are:

$$f^* = f + Y_{CO_2}/Y_{CO_2,air},\quad Y_{CO_2}^* = Y_{CO_2}/(fY_{CO_2,fuel}), \tag{4}$$

where $Y_{CO_2,fuel} = nM_{CO_2}/M_{C_NH_M}$, $Y_{CO_2,air} = M_{CO_2}/(M_{O_2} + M_{N_2}/0.259)$.

The local PDF is of the form:

$$P(f^*, Y_{CO_2}^*) = \exp[a_1 + a_2 f^* + a_3 Y_{CO_2}^* + a_4 f^{*2} + a_5 Y_{CO_2}^* + a_6 f^* Y_{CO_2}^*], \tag{5}$$

where f^* and $Y_{CO_2}^*$ are appropriately transformed variables and are calculated through the coefficients $(a_1 \ldots a_6)$ which depend on the local moments $\overline{f'^2}, \overline{Y_{CO_2}'^2}, \overline{f'Y_{CO_2}'}$ which are obtained assuming equilibrium between the turbulent production and destruction of these moments in their general form transport equation:

$$\frac{\partial\left(\overline{\rho}\,\overline{X'Z'}\right)}{\partial t}+\frac{\partial\left(\overline{\rho}\widetilde{u}_j\,\overline{X'Z'}\right)}{\partial x_j}=\frac{\partial}{\partial x_j}\left[\left(\overline{\rho}D+\frac{\mu_t}{Sc_t}\right)\frac{\partial\,\overline{X'Z'}}{\partial x_j}\right]+2\frac{\mu_t}{Sc_t}\left[\frac{\partial\widetilde{X}}{\partial x_i}\frac{\partial\widetilde{Z}}{\partial x_i}\right]$$
$$-C_\Phi\overline{\rho}\frac{1}{\tau_t}\overline{X'Z'}+\overline{X'S_Z}+\overline{Z'S_X}\ . \tag{6}$$

The moments are then obtained from the following expression:

$$\overline{X'Z'}=\frac{1}{2.0\overline{\rho}}\left[\frac{2\mu_t}{S_{Ct}}\frac{\partial\widetilde{X}}{\partial x_i}\frac{\partial\widetilde{Z}}{\partial x_i}+\overline{X'S_Z}+\overline{Z'S_X}\right]\tau_t,$$
$$\overline{X}=<\widetilde{f}>\ or\ <\widetilde{Y}_{CO_2}>\ \text{and}\ \overline{Z}=<\widetilde{f}>\ or\ <\widetilde{Y}_{CO_2}>,\ C_\Phi=2.0. \tag{7}$$

Mean quantities and correlations are evaluated by using PDF information e.g.

$$\tilde{\dot{r}}_{CO_2} = \frac{1}{\rho}\iint \tilde{\dot{r}}_{CO_2} J\rho P(f^* \tilde{Y}^*_{CO_2}) df^* dY^*_{CO_2}, \tag{8}$$

where J is the Jacobian of the transformation, τ_t is evaluated as follows in line with the hybrid model formulation: if $L_t > \Delta$ then $\tau_t = \Delta / \sqrt{<\tilde{k}>}$ and if $L_t < \Delta$ then $\tau_t = <\tilde{k}> / <\tilde{\varepsilon}>$.

2.2. Aerodynamic model

The reacting flows were calculated with the time-dependent N-S equations governing the temporal and spatial variation of the velocities and pressures e.g. $u = <u> + u'$ with $<u> = \bar{u} + u''$ where u and $<u>$ are the instantaneous and phase-averaged (or resolved) velocities, $\bar{u}$ and u'' are the time-mean and large-scale (resolved) fluctuating components and u' is the stochastic (subgrid) turbulent fluctuation. The model description given below closely follows the formulations adopted in [12]. For the reacting flows density-weighted values are used i.e. $<\tilde{f}> = \overline{\rho < f >} / \bar{\rho}$. The equation set may be written as follows:

$$\frac{\partial \bar{\rho}}{\partial t} + \frac{\partial \langle \tilde{u}_i \rangle}{\partial x_i} = 0, \frac{\partial \langle \tilde{u}_i \rangle}{\partial t} + \langle \tilde{u}_j \rangle \frac{\partial \langle \tilde{u}_i \rangle}{\partial x_j} = -\frac{1}{\rho}\frac{\partial \bar{\rho}}{\partial x_i} + \frac{\partial}{\partial x_j}\left[\nu \frac{\partial \langle \tilde{u}_i \rangle}{\partial x_j} - \langle u_i' u_j' \rangle \right] + (\bar{\rho} - \rho_\infty) g_i \tag{9}$$

with the Reynolds stresses obtained from the standard eddy-viscosity formula:

$$-<\overline{u_i' u_j'}> = <\tilde{\nu}_t> \left(\frac{\partial <\tilde{u}_i>}{\partial x_j} + \frac{\partial <\tilde{u}_j>}{\partial x_i} \right) - \frac{2}{3}\left[<\tilde{\nu}_t> \frac{\partial <\tilde{u}_i>}{\partial x_i} + <\tilde{k}> \right] \delta_{ij}. \tag{10}$$

In the conventional $k-\varepsilon$ model $<\tilde{\nu}_t>$ is related to the turbulence energy $<\tilde{k}>$ and its dissipation rate $<\varepsilon>$ as $<\tilde{\nu}_t> = C_\mu <\tilde{k}>^2 / <\varepsilon>$ where $<\tilde{k}>$ and $<\varepsilon>$ are obtained from the standard transport equations:

$$\frac{\partial}{\partial x_j}(U_j k) = \frac{\partial}{\partial x_j}\left(\frac{\nu_t}{\sigma_k} \frac{\partial k}{\partial x_j} \right) - \overline{u_i u_j} \frac{\partial U_i}{\partial x_j} - \varepsilon, \tag{11}$$

$$\frac{\partial}{\partial x_j}(U_j \varepsilon) = \frac{\partial}{\partial x_j}\left(\frac{\nu_t}{\sigma_\varepsilon} \frac{\partial \varepsilon}{\partial x_j} \right) - C_{\varepsilon 1} \frac{\varepsilon}{k} \overline{u_i u_j} \frac{\partial U_i}{\partial x_j} - C_{\varepsilon 2} \frac{\varepsilon^2}{k}, \tag{12}$$

where $C_\mu = 0.009$, $C_{\varepsilon 1} = 1.44$, $C_{\varepsilon 2} = 1.92$, $\sigma_\kappa = 1.0$, $\sigma_\varepsilon = 1.3$.

The standard $k-\varepsilon$ model has been formulated and tested within steady-state calculation procedures against a range of plane shear flows with no distinct peaks in their energy spectrum. When a 2D time-dependent calculation is used part of the energy spectrum is directly resolved by this type of calculation. There is clearly ambiguity as to whether the standard model is capable of partitioning (correctly or not at al) the total stress into its stochastic and periodic contributions.

In the present time-dependent calculations the spatial filtering due to the employed mesh is also accounted for in an effort to distinguish the directly computed (albeit 2D) turbulent motions, which are resolved by the mesh of size $\Delta = (\Delta x \Delta y)^{1/2}$, from the turbulence already

modeled by the $k-\varepsilon$ model. $<\tilde{\nu}_t>$ is therefore here evaluated by borrowing the Smagorinsky mixing length model from the large–eddy simulation (LES) formalism and the hybrid turbulence model is:

$$<\tilde{\nu}_t>=(C_s\Delta)^2\left(2<\tilde{S}_{ij}><\tilde{S}_{ij}>\right)^{1/2}, \text{ if } \quad L_t=\frac{<\tilde{k}>^{3/2}}{<\tilde{\varepsilon}>}>\Delta \quad \text{and}$$
$$<\tilde{\nu}_t>=C_\mu<\tilde{k}>^2/<\tilde{\varepsilon}>, \qquad \text{if} \quad L_t<\Delta. \tag{13}$$

C_s is taken as 0.1. The resulting $\tilde{\nu}_t$ is fed back into the production of $<\tilde{k}>$ in the $k-\varepsilon$ equations thereby producing a continuous distribution of $\tilde{\nu}_t$. The implicit scheme used here, is therefore well suited for this hybrid formulation. Calculations with the standard $k-\varepsilon$ model have been proven clearly inferior to the recent hybrid method predictions both for cold and reacting bluff-body flows, as has been demonstrated in *Koutmos et al*. [12].

2.3. Turbulent flame noise model

For the evaluation of the autonomous sound radiation due to the interaction of the turbulent fluctuations with the flame front the model formulation of *Klein*, [5] has been followed closely. Starting from the basic wave equation for low Mach number flows the one-dimensional sound generated by the fluctuating heat release from a turbulent non-premixed flame is evaluated by deriving an integral expression assuming that the instantaneous combustion zone is infinitely thin and that combustion is fast and determined by the mixing of fuel and air. The sound spectrum can then be expressed as a function of a turbulence spectrum (of assumed shape) of the mixture fraction at the flame front. The resulting expression for the sound spectrum for a non-premixed turbulent flame is then given in integral form as function of frequency:

$$pp(f_\nu)=2\pi\left(\frac{C_0}{S}\right)^2\iint_X\left[(\rho DBA)^2\frac{L_{cor}\theta_{f_\nu}}{2U}E_{ID}^2\left(\frac{2\pi f_\nu}{2U}\right)\right]dxdy, \tag{14}$$

where C_0 is the speed of sound, S is the area of combustor nozzle, D is the laminar diffusion coefficient, $B=\frac{1}{2}x/\frac{1}{\pi}D\int_0^\infty E_{ID}(k)dk$, $x=2.0\frac{\varepsilon}{k}\tilde{f}'^2$ is the scalar dissipation, f_ν is the frequency and E_{ID} is the one-dimensional turbulence spectrum of assumed shape:

$$E_{ID}=\begin{Bmatrix}1, & k_1<k_\varepsilon\\ (k_1/k_2)^{-(5/3)}, & k_\varepsilon<k_1<k_{kol}\\ 0, & k_1>k_{kol}\end{Bmatrix}$$

with $k_1=2\pi f/2U$, $k_\varepsilon=\pi/l_t$, $k_{kol}=\left(\varepsilon/\nu^3\right)^{1/4}$, $\theta_f=1\Big/\sqrt{(\nabla f)^2}$ is the thickness of the mixing layer between fuel and air, $A=[T_{flame}-T_0]/[T_{flame}f_{st}(1-f_{st})]$.

The parameter sound pressure level, *SPL*, expressed in dB can also be evaluated as:

$$SPL(f_\nu) = 20\log\left(\frac{\sqrt{pp(f_\nu)}}{20\cdot 10^{-6}}\right). \quad (15)$$

The time-averaged information about the turbulence sound spectrum and other parameters required in the above expression is derived from the basic reacting flow calculation and the computation of the sound spectrum is performed in a post-processing step.

2.4. Computational domain

The coflowing methane-air jet configuration and computational domain are shown in Fig. 1. The convective condition $\partial\phi/\partial t + U_0(\partial\phi/\partial t) = 0$, $(C = \overline{U}_0)$ was used at the outlet. A mesh of 205×123 (x, y) grid points was used with an axial expansion ratio of 1.1. For inlet conditions fully developed flow was assumed.

The equations were solved with a finite-volume method based on a staggered mesh, a pressure correction method (SIMPLE) and the QUICK differencing scheme [12]. A second-order scheme was used for temporal integration.

Time steps were of the order $10^{-4}\ldots10^{-5}$s depending on fuel Reynolds number. After an initial transient of about $30t_0$ $(t_0 = D/U_0)$ statistics were computed over approximately $100t_0$.

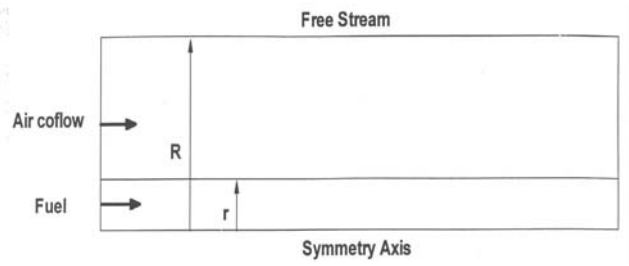

Figure 1.

Methane-air co-flowing jet flame configuration Investigated R=27r and the length of computation Domain is 50r

3. RESULTS AND COMPARISON

3.1. Aero-thermodynamic parameters

Computations were initially performed for a steady-state, laminar CH_4-air diffusion flame for which experimental data by Meier, et al. [14] is available. Figure 2 shows sample results for undiluted CH_4 jet flow at 5 cm/s through a 1.2 cm-diameter tube, with a co-flow of air at 10cm/s which are compared against the experimental data of reference [14].

Results are compared with data at the final steady-state which was reached at about 25.000 time-steps (Δt = 0.06 s). Overall the agreement is satisfactory in both the reactive scalar (temperature) and the momentum field (axial velocity) despite some experimental uncertainties concerning the rig exit conditions and these comparisons lend support for an extension of the basic model to the more complex turbulent diffusion flames.

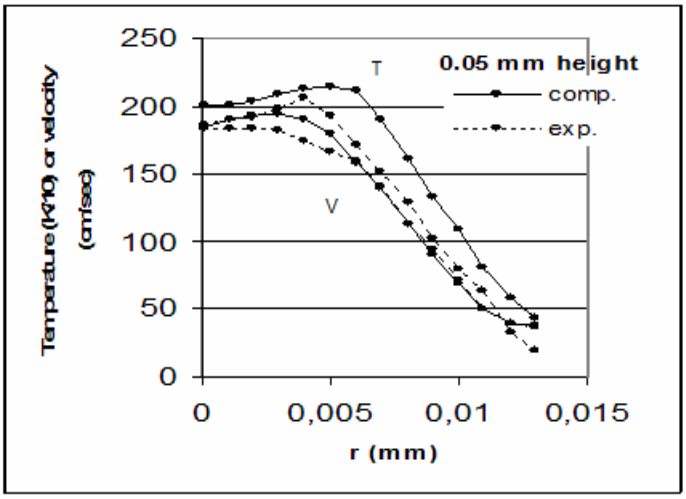

Figure 2. Laminar CH_4 jet flame predictions for fuel jet velocity 2 m/s

Figure 3 displays time-averaged temperature contours for jet velocity of 2 m/s investigated. The stoichiometric contour is also superimposed on the plot.

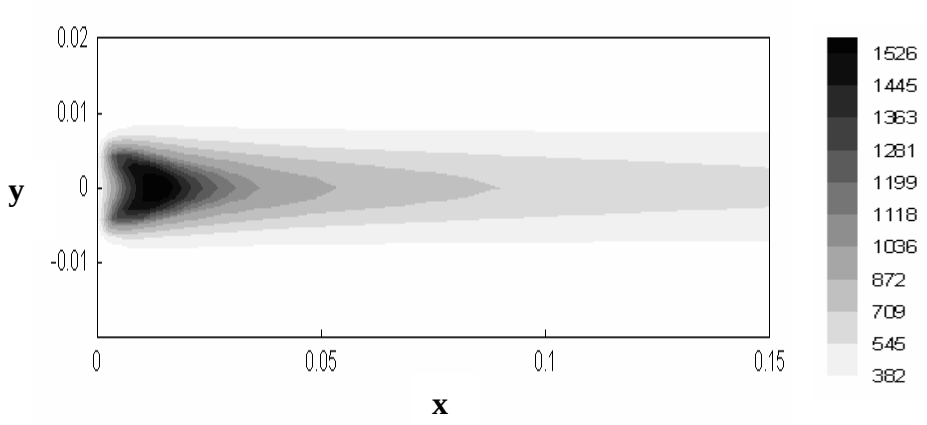

Figure 3. Time-averaged temperature contours for fuel jet velocity 2m/s

The distribution of temperatures of flame, of type of beam, constitutes perhaps the more basic characteristic. In the particular experiment the temperature was measured in order to it can be connected then with the under measurement sizes: the length and the intensity of sound of flame but also it is developed for the certification of calculating results. The measurements of temperature became with a step of order of 2 mm/s at length but also across the flame. This step is satisfactory for an experiment, of this order, after it can give us a completed picture in but also outside from the file of flame.

Certain indicative results for this case are given in Figure 4 where the actinic (radial) measurements of temperature in six different places at length of flame are presented. With

increase of benefit of fuel is observed increase of temperature at length of axis Z (vertical distance from the orifice of boiler). This increase becomes with decreased rate. This make is owed in that near in the boiler the flame is cold because excess fuel. Then the mixture is continued to the stoichiometric proportion. It was observed also that as long as they are increased the values of z increases the temperature of flame and becomes more emission of radiation. The temperature is stabilised round a marginal value in removed point of axis of flame. This happens because are minimised the intensity of turbulence (is decreased the speed of flow) and the flame become more laminar approaching her final value of temperature.

The lower temperatures prevail near the axis symmetry. As the points of measurement are removed by this (across) the temperature are increased and it reaches her biggest value in the limit of flame where they become chemical reactions.

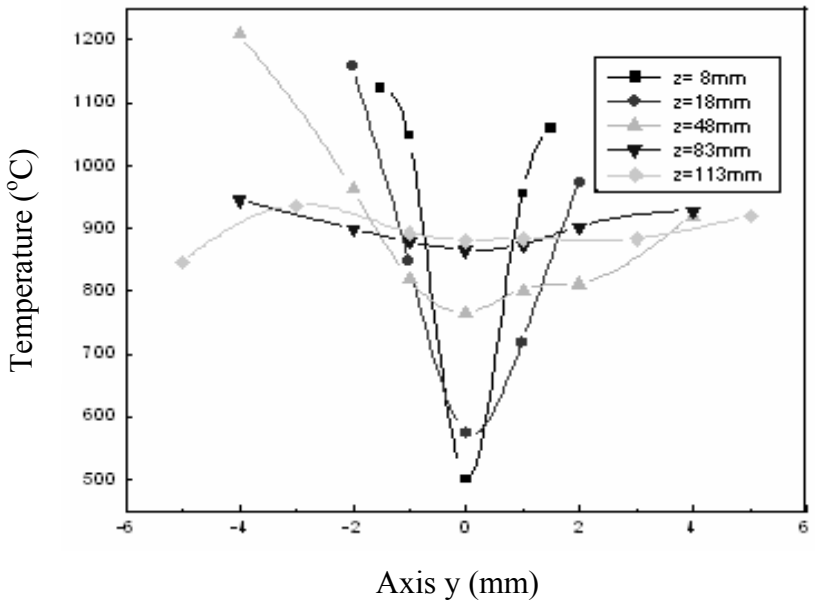

Figure 4. Temperature measurements in six different positions z along the flame length in the case of the **attached** flame

Apart from the case of the attached flame (figure 4) measurements was held for a lifted turbulent diffusion flame. The fuel was exited from a pipe, of diameter d = 0.96 mm. The velocity of air in the exit was the same as in the case of attached 1 m/s while the fuel velocity was 15 m/s so as to achieve the lift-off of the flame. In figure 5 the radial measurements of temperature for the lift-off flame in six different positions (z) along the flame length are presented.

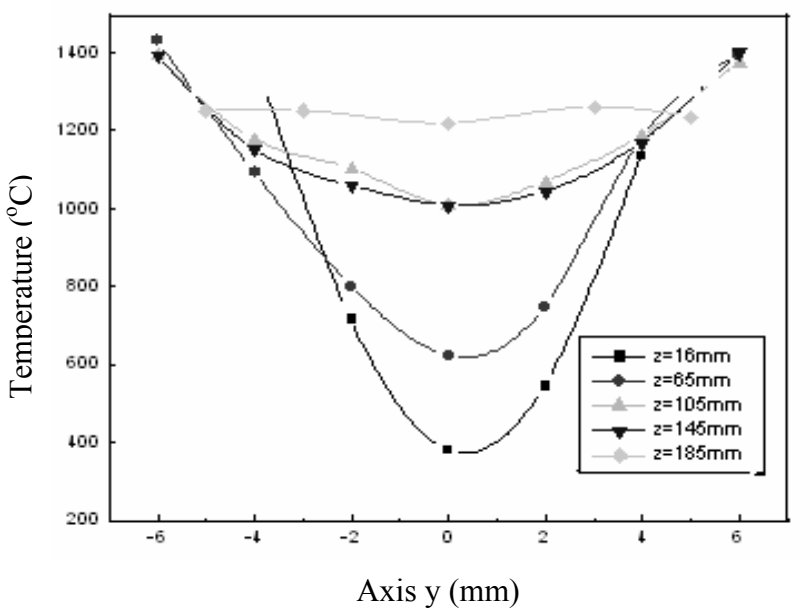

Figure 5. Temperature measurements in six different positions z along the flame length in the case of the **lifted** flame

Some preliminary joint statistics between temperature and mixture fraction, two important scaling parameters for the partially premixed regime have been produced from the time-dependent calculation for the higher fuel jet velocity of 20 m/s [15]. The collected points lie close to the stoichiometric contour in the vicinity of the movement of the flame base.

Propane is well known for its bimodel approach to extinction from a wide range of previously reported works (e.g [16]). The plot implies a lower level of bimodality with the scatter points located mostly above the mixing asymptote and below the partial equilibrium levels. The variance of mixture fraction spreads the points over an area slightly broader than the lean limit.

Experimental data of this nature would be very helpful in identifying the detailed nature and flow behavior of the near stabilization region. The reduced bimodality with respect to customary diffusion flames may be attributed to loss of resolution in the present simulation, to deficiencies in the reignition model which is formulated for pure diffusion flames, or to a lower variability of the chemical time-scale arising from omission of the effects of partially premixed flame propagation. This aspect which is not treated explicitly in the model other than through the inclusion of the relevant chemical time-scale.

Encouragingly the present modeling formulation recovered two important experimentally observed trends. Firstly, the linear relationship between flame lift-off height and jet exit velocity that has been extensively verified through global and detailed measurements as well as the correct slope of this linear variation. Secondly it reproduced adequately the increase in lift-off height for a given jet inflow velocity as the fuel flow is diluted e.g. with N_2, something expected since the residence time is now longer when the fuel stream is diluted.

3.2. Combustion noise (roar)

The reasonable performance of the computational model for the prediction of the experimentally observed aero-thermodynamic parameter variations and trends lends support to the extension of the method to include and apply the flame noise described previously to enable a meaningful evaluation of the combustion noise radiated by the present flames. Flame noise calculations have performed for two selected flame configuration, the attached flame with exit fuel velocity of 2 m/s in present work and the lifted-off flame by *Marazioti* [15] with exit fuel velocity of 20 m/s.

Equation (14) was discretized to be able to calculate it numerically and the integral is computed numerically at every grid cell. The part in square brackets of Eq. (14) can be considered as the strength of the local noise source and gives an indication of the spatial distribution of the local noise 'intensity' in the reacting flow field for each selected frequency.

Integrating numerically Eq. (14) for all cell volumes and over the full frequency range (Δf = 1 Hz, P_{ref} = 20 μPa) we deduce the sound spectrum expressed in dB sound pressure level from Eq. (15). The turbulent aero-thermochemical data produced by the basic time-dependent computation are time-averaged and supply the required information to evaluate the parameters involved in Eq. (15) for every cell volume and frequency. Figure 6 (a, b), for comparison, display contours of the local noise intensity (the term between the square brackets in Eq. (14)), attached and lifted [15] diffusion flame, for a frequency of 100 Hz.

It is seen that noise generation levels are predominant mainly in the vicinity of the mixing interface between fuel and oxidizer. These attain maximum values downstream of the lifted-off flame base for the lifted flame and the location of the maximum noise intensity coincides with the region of the peak temperatures levels.

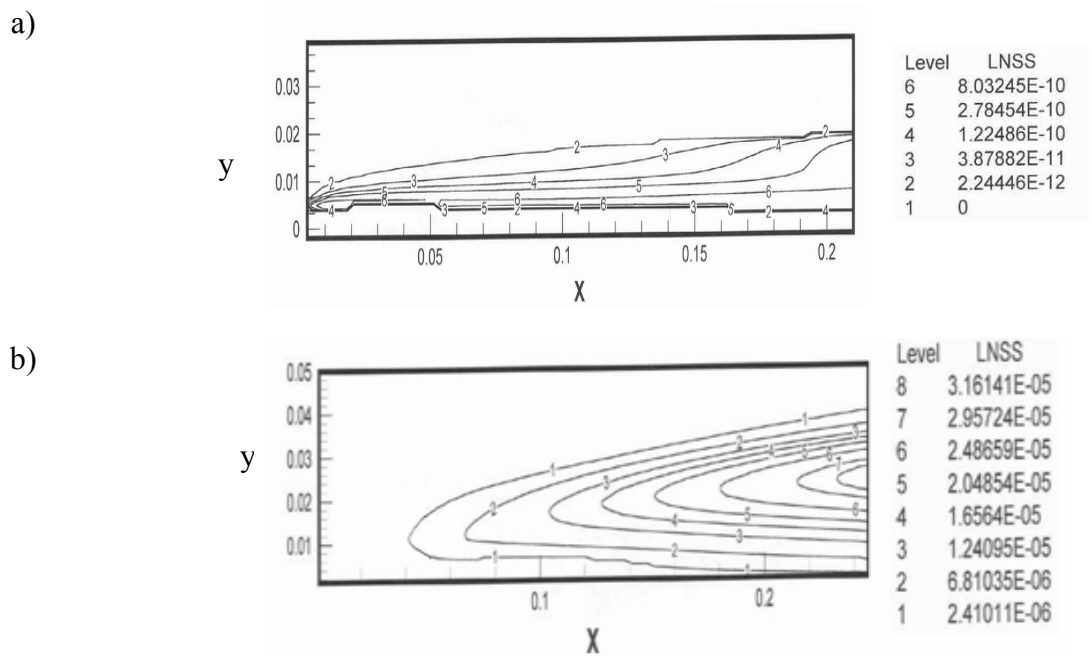

Figure 6. The local noise source intensity (LNSS) distribution for fuel jet velocity a) 2 m/s and b) 20 m/s [15] along the flame length: x-axis is the flame length and y-axis the flame width

The lifted flame produces significantly increased maximum values of the local noise source strength and this appears a reasonably predicted trend since the lifted flame produces increased turbulence levels and temperature fluctuations downstream of its lifted base.

The calculated sound spectra for the booth diffusion flame are plotted in Figure 7. The lifted flame gives elevated energy content in the sound spectrum and the difference in the noise level is about 40 dB at most frequencies and more near the frequency 80 Hz.

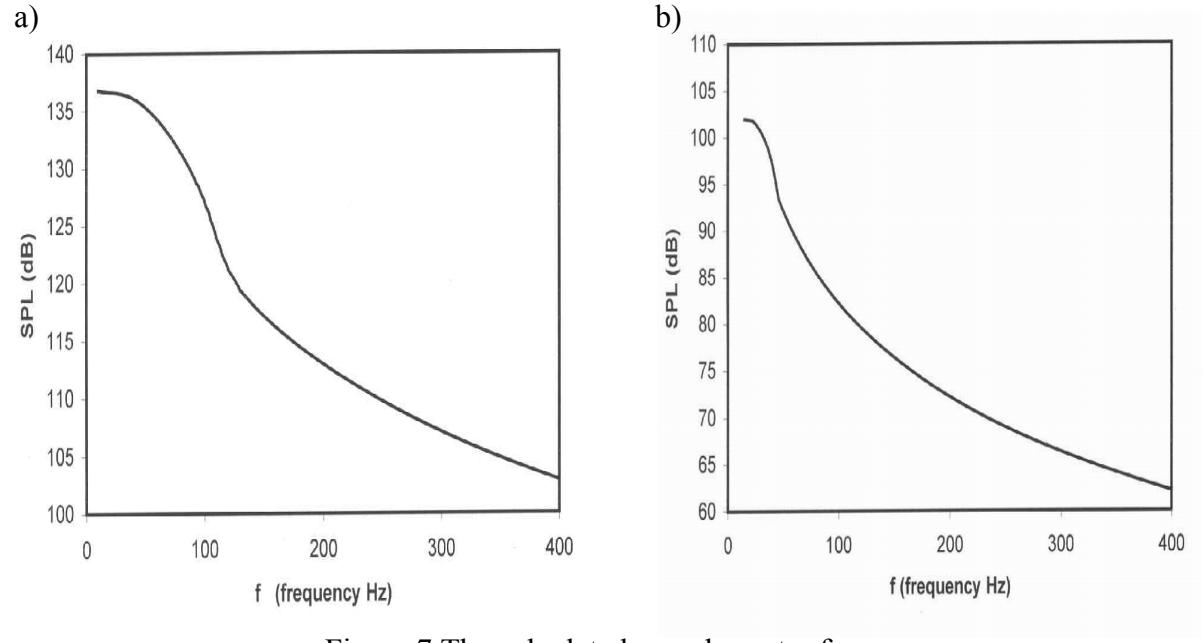

Figure 7.The calculated sound spectra for:
a) lifted [15] and b) attached flame, plotted in SPL dB (Δf=1 Hz)

This is evidently consistent with the previously discussed predictions of the local noise intensity levels. It should also be noted that the qualitative distribution of the spectral density also depends on the assumed turbulence spectrum used in Eq. (14).

An aspect that merits discussion is whether the assumption of fast chemistry can still be applied for the partially-premixed flame configuration with lift-off and to what extend the expected discrepancies affect the validity of the present prediction [17]. Experimental results would be quite helpful to identify the extent of disagreement in the sound pressure level predictions of this flame and this would help improve the present effort.

Note with standing the above arguments, it is believed that the present procedure has captured the basic behaviors and trends in the aero-thermochemical and flame noise generation characteristics of the studied flames although further tests and refinements would be required to enlarge the applicability of the method.

4. SUMMARY

A computational procedure the Large Eddy simulation turbulence model (LES) has been employed to study the stabilization mechanism and the autonomous noise generation by the flame front due to turbulent fluctuations in attached and lifted propane jet turbulent diffusion flames. Although the method exploited primarily diffusion flame concepts with the effects of partial extinctions/reignitions embodied, it produced reasonable qualitative agreement with reported data. Despite the fact that these exploratory and preliminary computations are based on axisymmetric configurations and hence the three-dimentional or the non-symmetric turbulent behavior is excluded the present method captured many important trends and behaviors and allows for an evaluation and further development of the overall methodology. Further extensions along the line of addressing in a more clear-cut manner the impact of partial-premixing are also required.

The adequate accord between computations and experimental observation in the turbulent aerothermodynamic flow and flame parameters allowed a first attempt at evaluating the turbulent combustion noise (roar) characteristics of the complex flame configuration investigated here. The developed methodology provides a basis to address the coupled effects of turbulence interactions, heat release and chemistry, and the autonomous turbulent combustion noise generated at the flame front. These preliminary results suggest that the modeling procedure followed such complex behaviors as the variation of the flame lift-off height with fuel jet velocity and the accompanying increase in the radiated flame noise levels. Further detailed assessment and improvements of the described methodology may however be required to validate and demonstrate its wider applicability.

5. ACKNOWLEDGMENTS

The research was funded by the program “K. Karatheodori”, Epitropi Ereunon, University of Patras.

REFERENCES

1. Lighthill, M. J. On sound generated aerodynamically. I. General theory. Proc. Roy. Soc, A 211, 564–587, 1952.
2. Klein, S. A. and Kok, J. B. W. Sound generation by turbulent non-premixed flames. Combustion Science and Technology, vol. 149, 1999.
3. Singh, K. K., Frankel, S. H. and Gore, J. P. Effects of combustion on the sound pressure generated by circular jet flows. Journal of American Institute of Aeronautics and Astronautics, 41, 319–321, 2003.
4. Singh, K. K., Frankel, S. H. and Gore, J. P. Study of spectral noise emissions from standard turbulent non-premixed flames. Journal of American Institute of Aeronautics and Astronautics, 42, 931–936, 2004.
5. Klein, S. A. On the acoustics of turbulent non-premixed flames, PhD thesis, University of Twente, Enschede, The Netherlands, 2000.

6. Brick, H., Piscoya, R., Ochmann, M. and Koltzsch, P. Modelling of combustion noise with the Boundary Element Method and Equivalent Source Method. Internoise-2004.
7. P. Boienau, Y. Gerrais and V. Morice. An aerothermoacoustic model for computation of sound radiated by turbulent flames. Internoise-96, 495–508, 1996.
8. Chen, M., Herrmann, M. and Peters, N. Flamelet modelling of lifted turbulent CH_4/air and C_3H_8/air jet diffusion flames. Proc. Comb. Inst., 28, 167, 2000.
9. P. Koutmos. Damkohler number description of local extinction in turbulent methane jet diffusion flames. Fuel, 78, 623–626, 1999.
10. Schneider, C., Dreizler, A., Janicka, J. and Hassel, E. Flow field measurements of stable and locally extinguishing hydrocarbon-fuelled jet flames. Combustion and Flame 135, 185–190, 2003.
11. Kempf, A., Sadiki, A. and Janicka, J. Prediction of finite chemistry effects using large-eddy simulation. in Proc. Comb. Inst. 29, 2002.
12. P. Koutmos, C. Mavridis and D. Papailiou. Time-dependent computation of turbulent bluff-body diffusion flames close to extinction. International Journal of Numerical Methods for Heat and Fluid Flow, 9, 39–59, 1999.
13. Koutmos, P. and Marazioti, P. Identification of local extinction topology in axisymmetric bluff-body diffusion flames with a reactedness-mixture fraction presumed probability density function model. International Journal for Numerical Methods in Fluids, 35, 939–959, 2001.
14. Meier, W., Barlow, R., Chen, Y. and Chen, J. Raman/Rayleigh/LIF measurements in a turbulent $CH_4/H_2/N_2$ jet diffusion flame: Experimental techniques and turbulence-chemistry interaction. Combustion and Flame 123, 326–343, 2000.
15. Marazioti P. An aerothermoacoustic model for computation of the combustion noise (roar) radiated by lifted turbulent jet diffusion flames. Electronic journal “Technical Acoustics”, http://www.ejta.org, 2009, 8.
16. T. Echekki and J. H. Chen. The effects of complex chemistry on triple flames. NASA CTR manuscript, Proceedings of the Summer School, 217–233, 1996.
17. D. Papailiou, P. Koutmos, C. Mavridis and A. Bakrozis. Simulations of local extinction phenomena in bluff-body stabilized diffusion flames with a Lagrangian reactedness model. Combustion Theory and Modelling, 3, 409–431, 1999.